PNAS
www.pnas.org

Supplementary Information for

Neural signatures of attentional engagement during narratives and its consequences for event memory

Hayoung Song, Emily S. Finn, Monica D. Rosenberg

Correspondence:
Hayoung Song and Monica D. Rosenberg
Email: hyssong@uchicago.edu, mdrosenberg@uchicago.edu

This PDF file includes:

Supplementary Text S1. Behavioral experiment results.

Inter-subject synchrony of engagement ratings across runs

To assess the consistency of engagement ratings during different parts of the narratives, we calculated pairwise participants' response consistency for each of the three runs of *Paranoia* and two runs of *Sherlock*. The stimuli were segmented with interim breaks so that the procedure matched experimental runs of the previously collected fMRI studies. Consistency of engagement ratings increased over time for *Paranoia* (run 1 mean Pearson's r = .051 ± .285, run 2 = .406 ± .285, run 3 = .449 ± .375; repeated measures ANOVA: $F(2,418) = 116.20$, $p < .001$) but decreased over time for *Sherlock* (run 1 = .231 ± .231, run 2 = .119 ± .291; $F(1,135) = 14.47$, $p < .001$), suggesting that the degree to which engagement is shared across individuals is idiosyncratic to different stories and may depend on narrative content.

Button response frequencies upon changes in engagement

We investigated whether the frequency of participants' button press responses differed depending on their state of engagement. Changes in button-press frequency were calculated by recording whether a participant made a button-press at every moment of time (sampled at every TR duration). Button-press time-courses (vectors of 1s and 0s) were divided by each individual's total number of button presses to account for individual differences in response frequency. All participants' button response time-courses were summed and submitted to a sliding window analysis (selection of time window was the same throughout the manuscript; 40 TR = 40 s for *Paranoia* and 30 TR = 45 s for *Sherlock*, with a step size of 1 TR) to measure changes in response frequency over time. The sliding window-averaged button press time-course was then compared with the sliding window-averaged group-mean engagement time-course using Pearson's correlation. For both narratives, we observed that participants made relatively fewer button-press responses (i.e., changed their ratings less frequently) during periods of high engagement (*Paranoia*: r = -.586, $p < .001$; *Sherlock*: r = -.528, $p < .001$). The pattern of results remained consistent if button press data were not divided by each individual's total number of responses before summing across individuals (*Paranoia*: r = -.697, $p < .001$; *Sherlock*: r = -.604, $p < .001$). This relationship may have arisen because participants were absorbed in the narrative events which made them less likely to focus on a task, or because of a ceiling effect such that responses were maximized within the 1 to 9 Likert scale range. Despite this correlation, however, behavioral results indicate that participants were able to dynamically report their stimulus-related attentional engagement during narratives.

Supplementary Text S2. Results of dynamic inter-subject correlation (ISC) analysis: Robustness across selection of window sizes.

We tested whether the dynamic ISC results were robust across selection of different sliding window sizes. In the manuscript, we used sliding window sizes of 40 TR [= 40s] for *Paranoia* and 30 TR [= 45s] for *Sherlock* datasets (with step size and Gaussian kernel set constant at 1 TR and 3 TR respectively). In additional analyses, we tested sliding windows 80% and 120% of these lengths (i.e., window sizes of 32 TR [= 32s] and 48 TR [= 48s] for *Paranoia* and 24 TR [= 36s] and 36 TR [= 54s] for *Sherlock)*.

For *Paranoia*, dynamic ISCs in 17 out of 19 regions that were reported to be correlated with group-average engagement in the main text (non-parametric permutation test, two-tailed $p < .05$) were significantly correlated with engagement in all three selections of window size. Right insula lobe (VAN) [-38.9, -23.6, +0.9] and right middle cingulate cortex (VAN) [-7.1, -26.5, +33.8] were not selected at a smaller window size (32 TR), and right angular gyrus (DMN) [-48.6, +69.3, +27.1] was additionally selected at a larger window size (48 TR).

For *Sherlock*, all 21 regions reported in the main text were selected in all three choices of sliding window sizes. Left inferior frontal gyrus (FPN) [+44.0, -38.1, +13.3] was additionally selected to be significantly correlated with group-average engagement at a larger window size (36 TR).

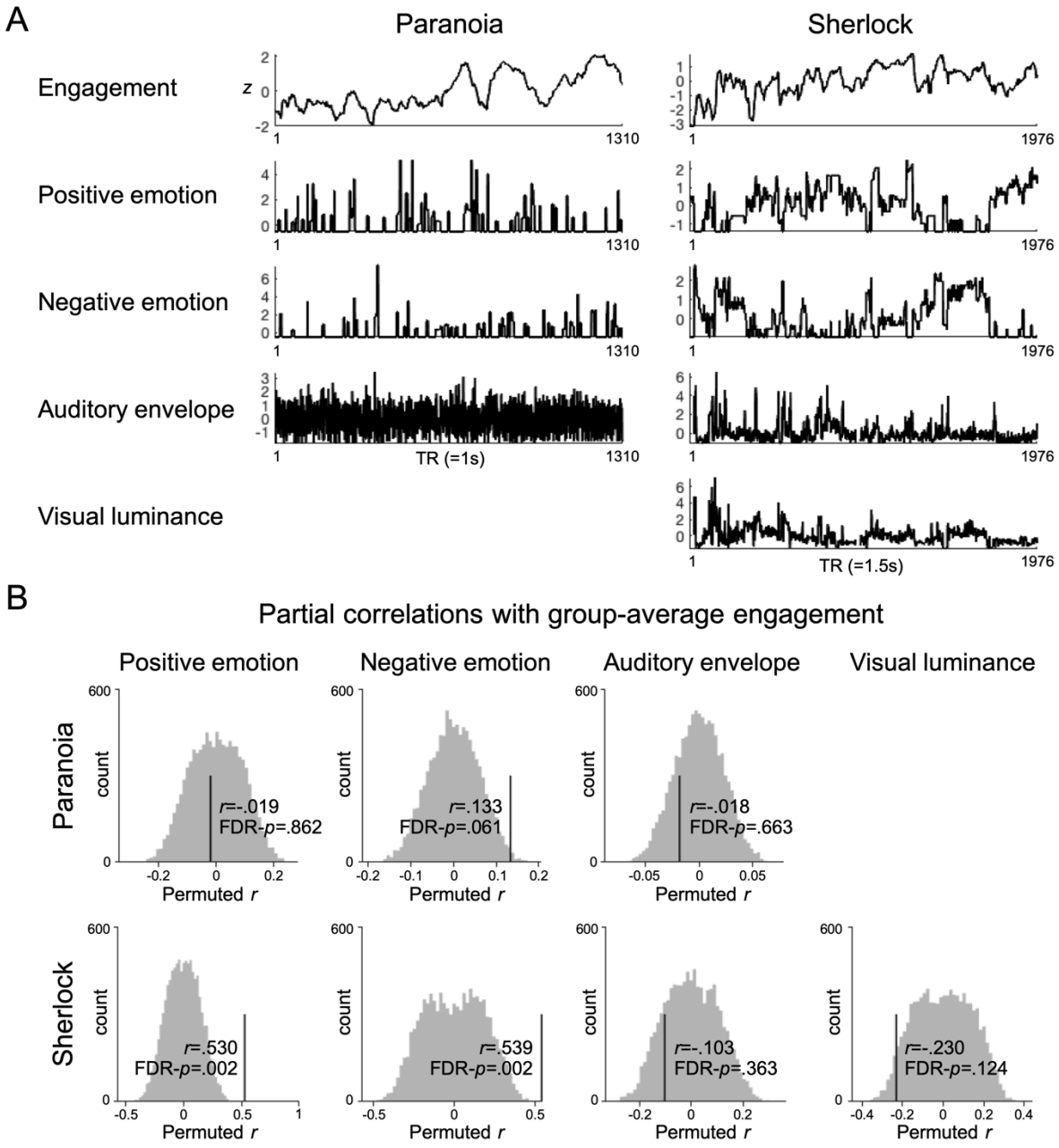

Supplementary Figure 1. Relationships between attentional engagement and multiple features of the narratives. (**A**) Time-courses of group-average engagement and four story components of *Paranoia* (left) and *Sherlock* (bottom). The time-courses were *z*-normalized across time. (**B**) Results of partial correlations between group-average engagement and each of the four story components, controlling for the other components, from the *Paranoia* (top) and *Sherlock* (bottom) datasets. Histograms indicate distributions of the null partial correlations with phase-randomized engagement ratings (iterations = 10,000). The lines indicate empirical partial correlation values, with the *p*-values indicating non-parametric, two-tailed significance tests. The significance of partial correlations was corrected for multiple comparisons within each narrative dataset.

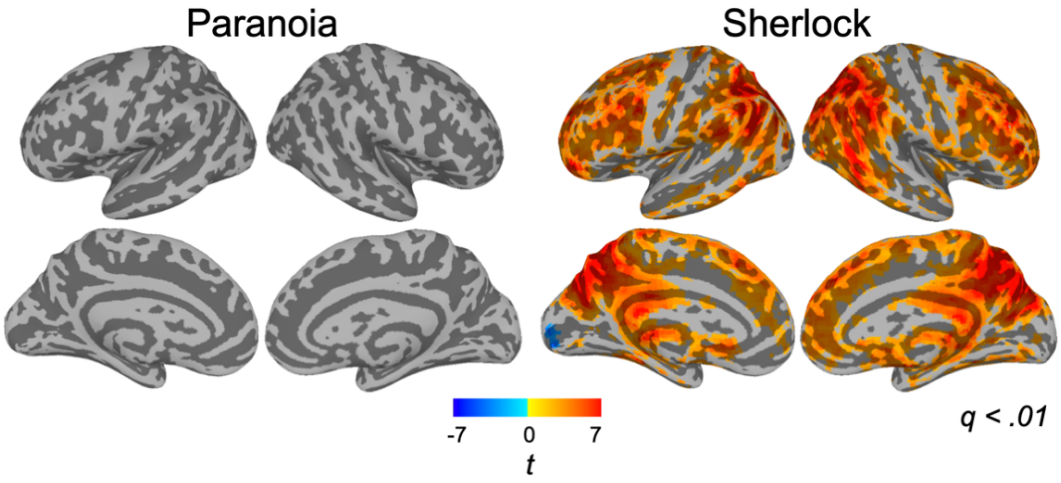

Supplementary Figure 2. General linear regression model (GLM) results relating group-average engagement time-courses to BOLD activity during *Paranoia* (left) and *Sherlock* (right) (cluster size = 35 and 44 voxels respectively, estimated from 3dFWHMx and 3dClustSim using AFNI; individual-voxel $p < .001$, cluster-corrected $\alpha < .05$). The auditory envelope and visual luminance were controlled for in the GLM. No region's activity was modulated by engagement in *Paranoia* ($q < .01$), whereas activity in almost every region, except somatosensory-motor and early visual and auditory regions, positively scaled with changes in *Sherlock* engagement (thresholded at $t(16) = 2.66$, $q < .01$).

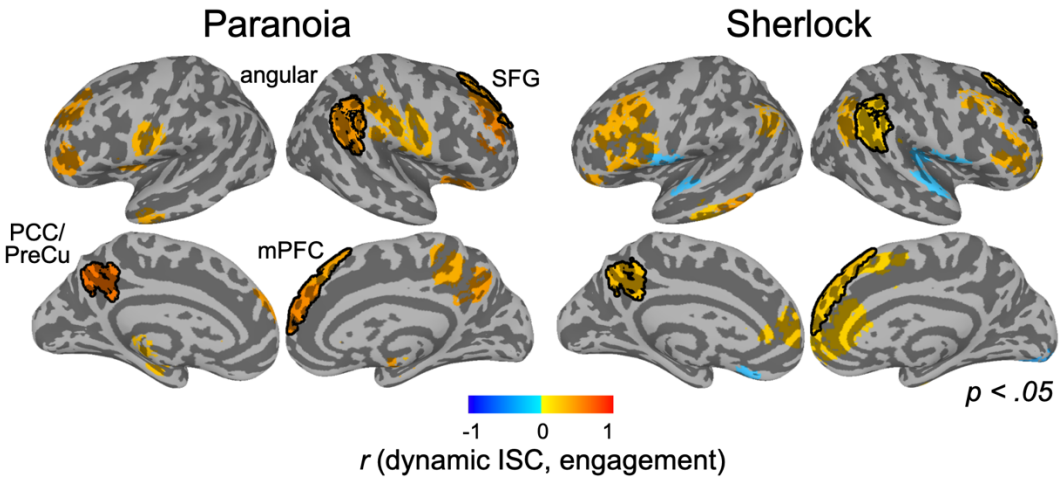

Supplementary Figure 3. Regions that show significant correlations between dynamic ISC and group-average engagement, using 268-ROIs Shen atlas (two-tailed test; uncorrected $p < .05$). 30 regions in *Paranoia* and 34 regions in *Sherlock* out of 268 total regions survived significance tests, with 29/30 regions in the *Paranoia* dataset and 29/34 regions in the *Sherlock* dataset exhibiting positive correlations between ISC and engagement. The ISCs of five regions–right superior medial gyrus [-8.5, -53.3, +23.9] ($r = .562$, $r = .281$ for *Paranoia* and *Sherlock* respectively), right superior frontal gyrus [-14.6, -36.7, +49.1] ($r = .434$, $r = .301$), left posterior cingulate cortex/precuneus [+6.4, +54.3, +37.4] ($r = .654$, $r = .339$), right angular gyrus [-54.2, +45.2, ++37.0] ($r = .490$, $r = .257$), and left cerebellum [+30.3, +80.1, -40.4] ($r = .454$, $r = .407$)–exhibited significant positive correlations with group-average engagement in both datasets. The overlap in a cerebellar region is not shown in the figure due to the cortical surface visualization. Angular: angular gyrus, mPFC: medial prefrontal cortex, PCC/PreCu: posterior cingulate cortex/precuneus, SFG: superior frontal gyrus.

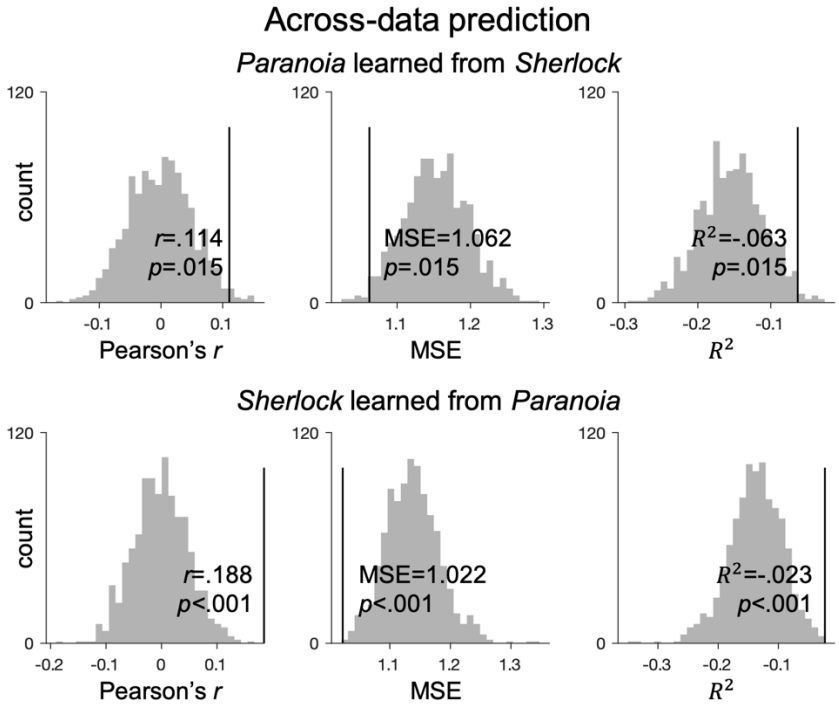

Supplementary Figure 4. Across-dataset prediction of group-average engagement from dynamic patterns of functional connectivity. The histograms indicate Pearson's *r* (left), MSE (center), and R^2 (right) values of null model performance that predicted phase-randomized engagement ratings (iteration = 1,000). The empirical values are indicated with vertical lines, with *p* values indicating one-tailed significance tests. Notably, both the null and empirical R^2 values are negative, and the empirical R^2 is consistently higher than chance. These results support our choice of Pearson's correlation between predicted and observed time-courses as an indicator of prediction performance, reflecting the degree to which models capture temporal dynamics rather than actual values at each moment of time.

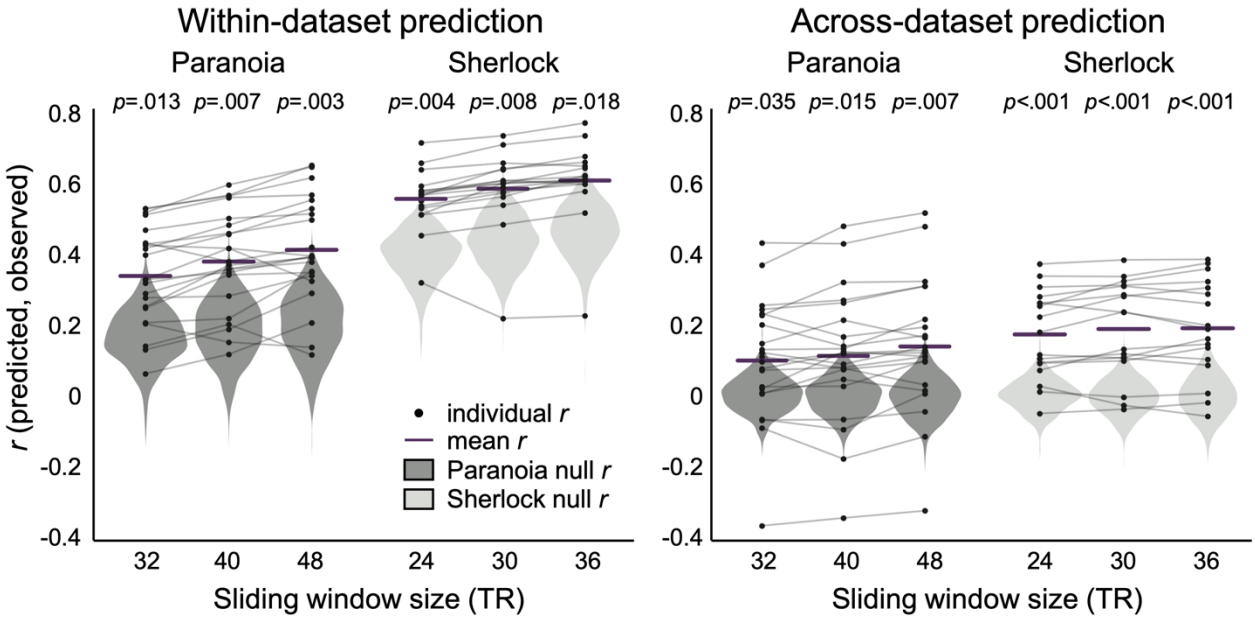

Supplementary Figure 5. Results of group-average engagement prediction from time-varying functional connectivity: Robustness across selection of window sizes. The results in the middle of each section (i.e., sliding window of 40 TR for *Paranoia* and 30 TR for *Sherlock*) correspond to the results shown in **Fig. 4A**. The trend of results was comparable when using different selection of sliding window sizes.

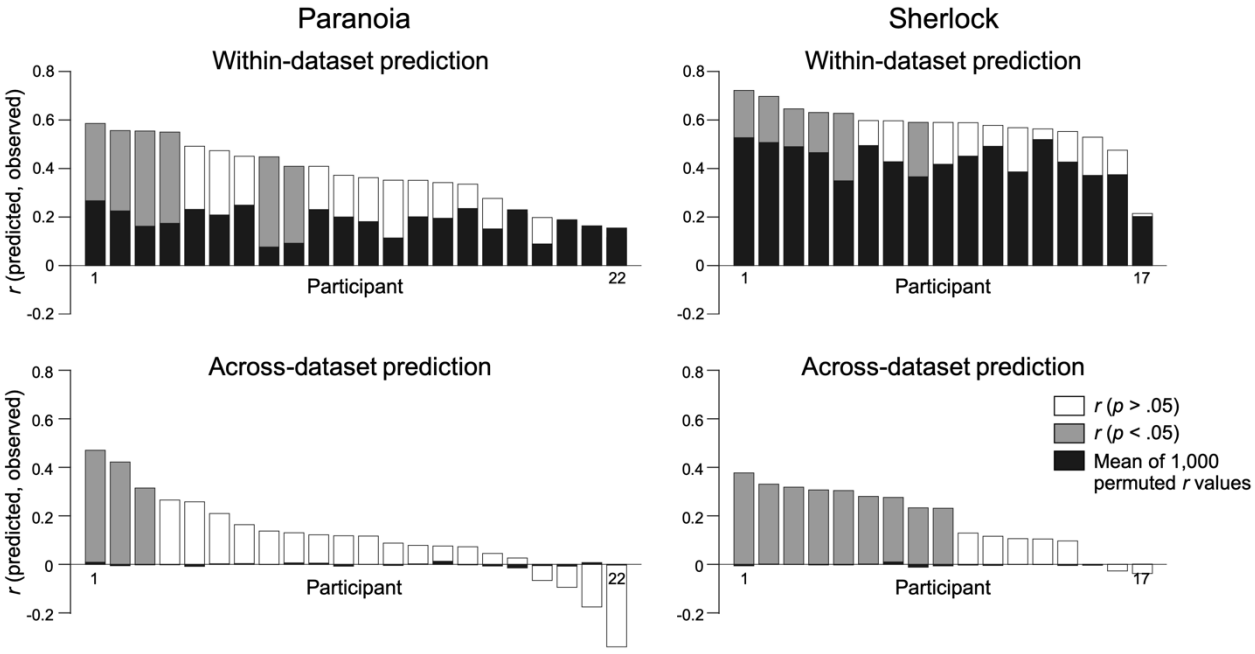

Supplementary Figure 6. Prediction of group-average engagement time-course from patterns of functional connectivity. Prediction results for every cross-validation fold of the within-dataset (top) and across-dataset (bottom) predictions, respectively for *Paranoia* (left) and *Sherlock* (right). The black bars indicate the mean of the 1,000 permuted correlation values per fold. Gray bars indicate observed correlations significantly greater than their corresponding null distribution (one-tailed test; uncorrected $p < .05$), and white bars indicate observed correlations which did not pass this significance threshold.

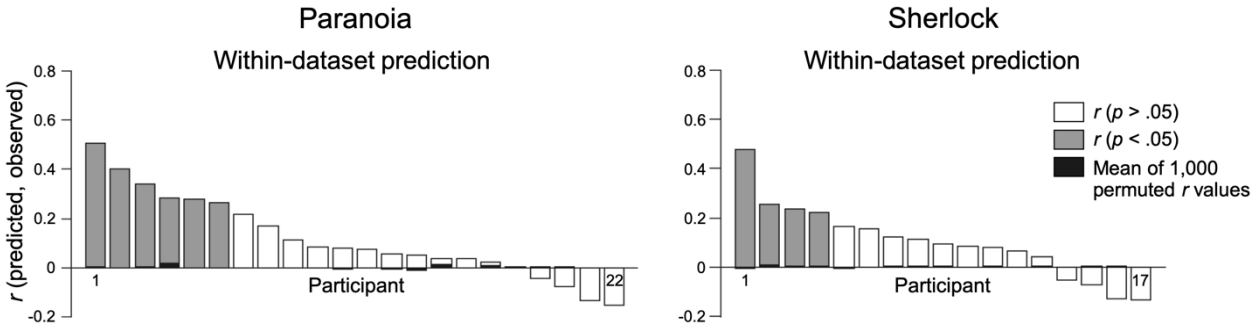

Supplementary Figure 7. Prediction of individual-specific recall fidelity time-course from the engagement network. Prediction results for every cross-validation fold of the within-dataset analysis for *Paranoia* (left) and *Sherlock* (right). The black bars indicate the mean of the 1,000 permuted correlation values per fold. Gray bars indicate observed correlations significantly greater than their corresponding null distribution (one-tailed test; uncorrected $p < .05$), and white bars indicate observed correlations which did not pass this significance threshold.

Positive emotion words

accept, adventure, amazingly, appreciated, appreciation, beautiful, best, better, calm, care, certain, comfortable, delicate, delicious, delight, eager, eagerly, enjoyed, enjoying, excited, festival, funny, giving, good, grateful, gratitude, great, happy, helping, hope, hoped, hoping, important, improved, interesting, luckily, okay, played, playing, please, pleased, pretty, promised, proud, ready, relief, rewarding, safely, smile, smiled, sure, surprised, thank, thrilled, truly, trusting, warm, welcome, welcoming, well, wonderful, would like, you like

Negative emotion words

afraid, alarmed, anxious, apprehensively, ashamed, avoiding, bad, bother, broke, confused, desperate, distrustful, embarrassed, empty, exhausted, fault, frightened, frustrated, guilt, guilty, homesick, horribly, interrupted, isolated, lonely, lost, missed, nasty, nervous, nightmares, panic, pressure, problems, risking, scared, shock, shocked, shook, shy, sick, sigh, sorry, startled, strange, struggled, tears, threatening, traumatized, uncomfortable, unsettled, victims, weak, worried, worse, yell

Supplementary Table 1. Lists of positively and negatively valenced words that appear in the *Paranoia* narrated transcript. We analyzed the Linguistic Inquiry and Word Count (LIWC; www.liwc.net) output of the *Paranoia* story transcript, provided by Finn et al. (2018; *Nat. Commun*.). The LIWC software takes every word in the story transcript as input and counts the number of words falling into different syntactic and semantic categories. The categories of interest were ‘positive emotion’ and ‘negative emotion’.

Paranoia

MNI coordinate			Dynamic ISC correlation with engagement		Functional Networks	Region
x	y	z	*r*	*p*		
+53.0	+8.8	+34.4	0.403	0.007	SM	Left Postcentral Gyrus
+16.5	-9.0	+69.0	0.405	0.016	VAN	Left Superior Frontal Gyrus
+32.1	-44.4	+28.2	0.452	0.017	VAN	Left Middle Frontal Gyrus
+44.0	-38.1	+13.3	0.475	0.008	FPN	Left Inferior Frontal Gyrus
+6.1	+51.0	+31.5	0.654	0.009	DMN	*Left Posterior Cingulate Cortex
+57.7	+12.2	-17.6	0.398	0.012	DMN	Left Middle Temporal Gyrus
-54.4	+6.0	+33.1	0.325	0.031	SM	Right Postcentral Gyrus
-48.4	+10.6	+15.1	0.469	0.034	SM	Right Rolandic Operculum
-51.9	-1.1	+48.0	-0.301	0.039	VAN	Right Precentral Gyrus
-13.2	-12.1	+67.3	0.521	0.016	VAN	Right Supplementary Motor Area
-32.1	-46.6	+28.4	0.585	0.008	VAN	Right Middle Frontal Gyrus
-46.3	-44.6	+2.5	0.421	0.028	VAN	Right Middle Frontal Gyrus
-38.9	-23.6	+0.9	0.462	0.049	VAN	Right Insula Lobe
-7.1	-26.5	+33.8	0.381	0.046	VAN	Right Middle Cingulate Cortex
-4.3	-35.0	+44.5	0.400	0.044	FPN	Right Superior Medial Gyrus
-61.3	+5.3	-17.3	0.449	0.006	DMN	Right Middle Temporal Gyrus
-50.9	+56.7	+29.7	0.454	0.008	DMN	*Right Angular Gyrus
-23.3	-36.5	+44.1	0.529	0.007	DMN	Right Superior Frontal Gyrus
-9.8	-49.2	+41.9	0.449	0.009	DMN	*Right Superior Medial Gyrus

Sherlock

MNI coordinate			Dynamic ISC correlation with engagement		Functional Networks	Region
x	y	z	*r*	*p*		
+51.6	+19.3	+6.8	-0.233	0.014	SM	Left Superior Temporal Gyrus
+56.6	+56.0	-13.6	0.434	0.023	FPN	Left Inferior Temporal Gyrus
+43.2	-13.5	+28.3	0.407	0.011	FPN	Left Inferior Frontal Gyrus
+60.0	+38.6	-13.7	0.377	0.011	FPN	Left Middle Temporal Gyrus
+48.8	+52.7	+49.8	0.408	0.041	FPN	Left Inferior Parietal Lobule
+43.1	-23.7	+40.4	0.398	0.039	FPN	Left Middle Frontal Gyrus
+4.5	-29.0	+46.8	0.322	0.042	FPN	Left Superior Medial Gyrus
+45.6	+67.8	+37.8	0.343	0.003	DMN	Left Angular Gyrus
+22.8	-28.2	+46.0	0.326	0.018	DMN	Left Middle Frontal Gyrus
+6.1	+51	+31.5	0.309	0.033	DMN	*Left Posterior Cingulate Cortex
+52.9	+55.5	+28.8	0.296	0.037	DMN	Left Angular Gyrus
+40.8	-13.6	+50.9	0.394	0.027	DMN	Left Middle Frontal Gyrus
+43.1	+76.6	+30.0	0.320	0.023	DMN	Left Angular Gyrus
-10.4	+96.2	-2.0	-0.351	0.020	VIS	Right Calcarine Gyrus
-53.7	+13.5	+5.5	-0.254	0.010	SM	Right Heschls Gyrus

-40.9	+48.3	+45.7	0.336	0.039	FPN	Right Inferior Parietal Lobule
-52.1	+51.0	+47.3	0.387	0.012	FPN	Right Inferior Parietal Lobule
-40.0	-19.9	+47.9	0.415	0.009	FPN	Right Middle Frontal Gyrus
-50.9	+56.7	+29.7	0.323	0.014	DMN	*Right Angular Gyrus
-7.5	-50.4	+5.7	0.314	0.003	DMN	Right Superior Medial Gyrus
-9.8	-49.2	+41.9	0.228	0.039	DMN	*Right Superior Medial Gyrus

Supplementary Table 2. Regions that show significant correlation between dynamic inter-subject correlation (ISC) and group-average engagement, visualized in **Fig. 2b** (uncorrected $p < 0.05$), of *Paranoia* and *Sherlock* stories, respectively. The center of mass of each ROI was extracted using AFNI, and its coordinates and label were annotated within the MNI space. The *r* values indicate Pearson's correlation of the ROI's dynamic ISC and group-average engagement. The *p* values indicate the comparisons of empirical *r* values to the null distribution where the engagement was phase-randomized (two-tailed test, uncorrected for multiple comparisons). *Asterisks indicate regions that were significant in both datasets.

Feature selection threshold	Sustained attention network # of FCs	Engagement network # of FCs	# of overlapping FCs	Significance of overlap (*p*-value)
.05	(+) 321, (-) 505	(+) 1193, (-) 229	(+) 80, (-) 21	(+) <.001, (-) .066
.01	(+) 134, (-) 200	(+) 583, (-) 102	(+) 20, (-) 1	(+) .002, (-) .769
.005	(+) 95, (-) 134	(+) 409, (-) 72	(+) 11, (-) 1	(+) .006, (-) .377
.001	(+) 45, (-) 56	(+) 201, (-) 24	(+) 2, (-) 0	(+) .123, (-) .167

Supplementary Table 3. Anatomical overlap of the sustained attention network and the engagement network defined from *Sherlock* dataset, across different feature selection thresholds. In every round of leave-one-subject-out cross-validation, we applied feature selection to select relevant functional connections (FCs) whose strength is correlated with individuals' behavioral scores (i.e., gradCPT performance) or select relevant FCs whose dynamic time-courses are correlated with behavioral time series (i.e., group-average engagement). The FCs correlated with behavior—either in the positive or negative direction—above significance threshold were selected. The FCs that were selected in every round of cross-validation were included in each network. We calculated the overlapping number of FCs showing the same directional correlations in the two networks. The main text uses a threshold of $p < .01$. The significance of anatomical overlap was computed using the hypergeometric cumulative distribution function. (+): positively correlated with behavior, (-): negatively correlated with behavior.